THE JOURNAL OF PHYSICAL CHEMISTRY B

ARTICLE

pubs.acs.org/JPCB

Generation and Recombination Kinetics of Optical Excitations in Poly(3-dodecylthienylenevinylene) with Controlled Regioregularity

Evan Lafalce and Xiaomei Jiang*

Department of Physics, University of South Florida, Tampa, Florida 33620, United States

Cheng Zhang

Department of Chemistry and Biochemistry, South Dakota State University, Brookings, South Dakota 57007, United States

ABSTRACT:

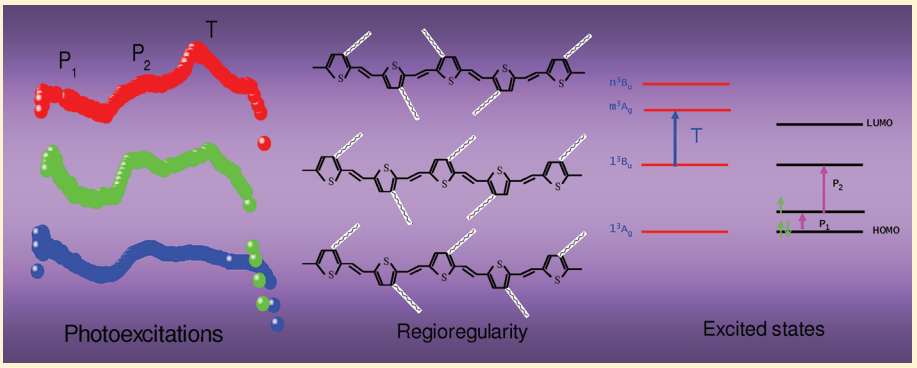

Regioregularity in π-conjugated polymers is known to have desirable effects on chain organization in the solid state leading to improved characteristics for electronic device applications. In this report, we studied the photophysics of a new series of π-conjugated polymers, namely, poly(3-dodecylthienylenevinylene), with controlled regioregularity (PTV-CR), using the steady state photoinduced absorption (PIA), doping-induced absorption (DIA), thermally modulated absorption (TMA), and photoluminescence (PL) techniques in a broad spectral range, as well as Grazing incidence X-ray diffraction (GIXRD). PTV-CR has a low band gap of 1.65−1.70 eV from the most random PTV-5:5 to regular PTV-0:10. We have found that regioregularity affects optical properties of PTV-CR in different ways than in the case of well-studied poly(3-alkylthiophene). We discovered that even the most random PTV-5:5 shows submicrometer crystalline order, and there is no correlation between regioregularity and crystallinity. We found that PTV is intrinsically *dark* due to the reverse order of $1B_u$ and $2A_g$ excitons, with PL quantum efficiency ranging from 10^{-5} to 2×10^{-4}. Spectroscopic data confirm the existence of long-lived neutral (triplets) and charged (polaron) excitations, and thus PTV is a *unique* nondegenerate ground state π-conjugated polymer which is intrinsically nonluminescent. The recombination mechanism and lifetime of such long-lived excitations are investigated through the pump intensity and pump frequency dependencies as well as temperature dependence of the sample. Increasing regioregularity is seen to reduce the thermal responsivity and intersystem crossing in these films. The novel, intrachain character of these effects and their implications for use of PTV derivatives for photovoltaic application are discussed.

INTRODUCTION

The class of materials known as π-conjugated polymers is currently under investigation for their interesting electronic and optical properties, as well as for their potential use in organic electronic devices. Notably, poly(3-hexylthiophene) (P3HT), an alkyl-substituted polythiophene derivative, has been successfully employed in organic photovoltaics (OPVs) and organic field-effect transistors (OFETs).[1−3] Additionally, derivatives of poly(phenylene vinylene) (PPV) have been widely used in OPVs and organic light-emitting diodes (OLEDs).[4,5] Poly(thienylenevinylene) (PTV) is a nondegenerate ground state conjugated polymer with a structure which is considered similar to polythiophene or PPV. It was recognized that the vinylene linkage between phenylene units as compared to the parent poly(*para*-phenylene) (PPP) led to a decreased band gap through a reduction in the aromatic resonance energy and enhanced electron delocalization.[6] In this regard, PTV may be considered the thiophene analogue of PPV. It indeed exhibits a lower optical band gap than polythiophene derivatives and could thus provide a better match with the solar spectrum in OPV application.[7,8] The oxidation potential of this polymer is low, in favor of stabilization of excitonic states.[9] Good hole mobility has been

Received: July 13, 2011
Revised: September 7, 2011
Published: September 14, 2011

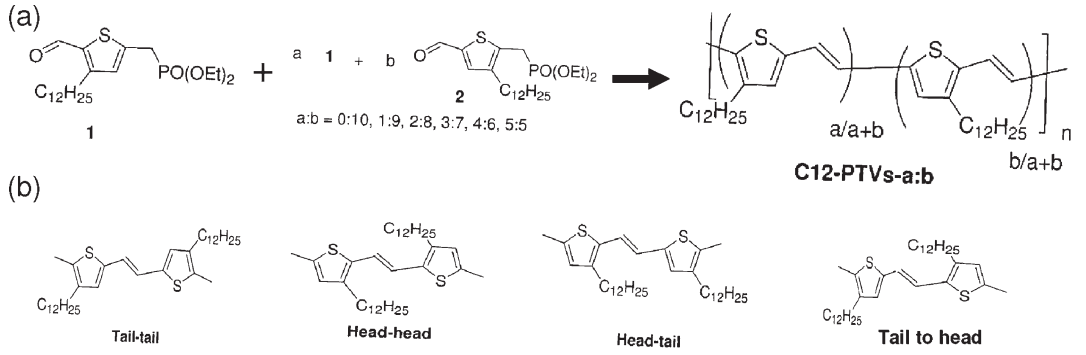

Figure 1. (a) Brief synthesis scheme and molecular structure of C12-PTVs-*a*:*b* (PTV-CR). (b) Four different configurations of two neighboring thiophene units: head−head (HH), tail−tail (TT), head−tail (HT), and tail−head (TH). The *a*:*b* ratio defines the regioregularity order, with 0:10 being 100% HT order (regioregular, RR-) and 5:5 being 25% HT ratio (regiorandom, RRa-).[23]

demonstrated in OFETs of PTV.[10] However, devices fabricated with this material so far have yielded very low efficiencies.[11−14] Electron transfer between these systems and C_{60} fullerene molecules has been suggested, although a study in the ultrafast regime suggests this process may be quite inefficient.[15,16] It is currently unclear whether the low efficiencies observed in PTV-based solar cells to date are due to poor charge transfer or other unknown reasons, and more detailed optical and structural investigations need to be conducted to realize the potential of this polymer.[14,17,18]

Regioregularity (RR) has been shown to improve the crystallinity of solution cast films of poly(alkylthiophenes) with respect to their regiorandom (RRa) counterparts.[19] This increases the strength of interchain interactions and results in higher mobility[20] and a lower optical band gap,[21] both of which lead to improved performance in OPV application.[22] For the first time, a series of poly(3-dodecylthienylenevinylenes) with controlled regioregularity (PTV-CR) were synthesized via a Horner−Emmons reaction using two isomeric comonomers with molar ratios from 0:10 to 5:5.[7,23] Here, an optical investigation of PTV-CR, with controllable regioregularity from regiorandom PTV-5:5 (25% head−tail) to regioregular PTV-0:10 (100% head−tail) (see Figure 1), is presented as an attempt to obtain a better understanding of the photogenerated excited states and their respective recombination mechanisms. By studying the regioregularity effect of this novel series of PTVs, more can be learned about the microscopic arrangement and the subsequent balance of intrachain versus interchain coupling in π-conjugated polymer films. In particular, the photoinduced absorption (PIA) technique is employed to detect long-lived subgap states.[24] Through analysis of the intensity, frequency, and temperature dependence of the absorption associated with these states, much has been learned about the decay mechanisms for photogenerated excitons in this interesting material. Combined with doping-induced absorption (DIA) and thermally modulated absorption (TMA), we hope to derive the regioregularity effect on the electronic levels in PTV-CR and thus help to improve the performance of PTV-based photovoltaic devices.

EXPERIMENTAL SECTION

1. Polymer Synthesis. Poly(3-dodecylthienylenevinylene) with controlled regioregularity (PTV-CR) was synthesized via the Horner−Emmons reaction between the aldehyde and phosphonate groups of difunctionalized comonomers **1** and **2** (Figure 1). **2** is synthesized according to previously established procedure.[7] Synthesis of **1** has been only recently accomplished.[23] The *a*:*b* ratio in Figure 1 defines the region-regularity order, with 0:10 being 100% head-to-tail (HT) ratio (regioregular, RR-) and 5:5 being only 25% HT ratio (regiorandom, RRa-). These two extremes and the intermediates 1:9, 2:8, 3:7, and 4:6, listed in order from regioregular to regiorandom, are studied here. The correspondence between *a*:*b* ratio and regioregularity was reported elsewhere.[23]

2. Sample Preparation and Measurements. PTV-CR was dissolved in dichlorobenzene solutions at 10 mg/mL by stirring on a hot plate at 90 °C for 24 h. The films for optical measurements were cast onto glass (for UV/visible range measurements) or sapphire (for visible/IR range measurements) substrates by drop casting or spin coating when thickness control was desired. Samples were allowed to dry for 24 h in a N_2 environment before measurements. Thickness measurement was performed by a Dektak profilometer, yielding values on the order of 100 nm for spun coat film and on the order of micrometers for drop cast film.

All optical experiments were conducted using a standard photoinduced absorption (PIA) setup.[25] An Ar^+ laser beam at $\hbar\omega$ = 2.5 eV modulated at various frequencies, *f*, was used for excitation, and an incandescent tungsten/halogen lamp was used as the probe. The PIA signal was measured using a lock-in amplifier referenced at *f*, a monochromator, and various combinations of gratings, filters, and solid-state photodetectors spanning the spectral range $0.3 < \hbar\omega$ (probe) < 2.7 eV. For thermally modulated absorption (TMA) and PIA experiments, films were mounted inside a Jannis coldfinger cryostat to provide temperature control down to 10 K. TMA difference spectra are calculated as $-\Delta T/T = (T(300\text{ K}) - T(10\text{ K}))/T(10\text{ K})$. The PIA signal is calculated as $-\Delta T/T = (T - T^{\text{pump}})/T$, where T^{pump} is the transmission measured while the pump excitation is incident on the sample, and T is the transmission without pump. For the range of chop frequencies used here (10 Hz to 1k Hz), processes that occur on a time scale of 100 μs to 10 ms can be detected. This setup was also used for measuring the PL spectrum, whereas the PLQE was measured with an integrated sphere.[26] For doping-induced absorption (DIA) measurements, we included some pieces of crystalline iodine in the same chamber of a PTV film for tens of seconds, where the doping with iodine (I_3^-) occurred by sublimation. DIA is obtained by calculating the difference spectra as $-\Delta T/T = (T - T^{\text{doped}})/T$.

Grazing Incidence X-ray Diffraction (GIXRD) was performed on a Phillips X-ray Diffractometer with a 1.54 Å X-ray source.

dx.doi.org/10.1021/jp2066666 |J. Phys. Chem. B 2011, 115, 13139–13148

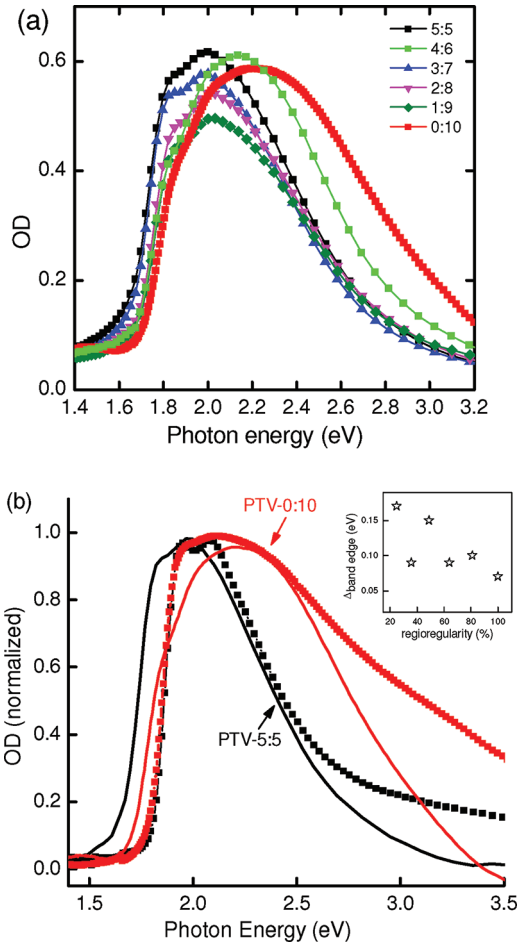

Figure 2. (a) Absorption spectra of films of PTV-CR and (b) comparison of absorption spectra of films (line) and solutions in DCB (line + symbol) of PTV-0:10 (regular, red) and PTV-5:5 (random, black). Inset shows the shift of band edge in film and solution versus regioregularity.

The incident angle was 1°, and the 2θ scan was performed in the axis perpendicular to the plane of the film. The drop cast films on sapphire substrates were used for these measurements, after subtracting the background signal from the bare sapphire substrate.

RESULTS AND DISCUSSION

1. Optical Absorption. In Figure 2a, the absorption spectra in films of the six PTV-CRs are shown together. The onset of absorption, or band edge, shows a blue-shift with increasing regioregularity. The band edge occurs at 1.61 eV for regiorandom PTV-5:5 and 1.70 eV for regioregular PTV-0:10. This indicates that the effect of regioregularity in PTV-CR is very different from the case for poly(3-hexyl)thiophene (P3HT), where a significant redshift of the absorption onset (~0.32 eV) from regiorandom (RRa-P3HT) to regioregular (RR-P3HT) was observed and explained by energy level splitting caused by the strong interchain interaction.[25] In the same case, it was found that the peaks due to the vibronic levels of the excited states could only be resolved in RR-P3HT, whereas the broader distribution of conjugation length in RRa-P3HT smeared out such structures.[21,25,27] The vibronic levels are apparent in the spectra of all PTV-CRs, with no correlation to regioregularity. As a matter of fact, the spectrum shape is more broad and featureless for regioregular PTV-0:10, which might be from inhomogeneity in PTV-0:10 film morphology since this polymer is the least soluble among the PTV-CR series.[7,23] Measurement of HOMO−LUMO levels in PTV-CR reveals that PTV-0:10 (regioregular) has a larger electronic band gap than that of PTV-5:5 (region-random) by 0.06 eV.[23]

As the optical gap of π-conjugated polymers is considered to be directly related to the conjugated length, the average conjugation length in these films may be estimated by comparison with *n*TV oligomers.[15,28] It appears the conjugated segment extends to 10−12 monomers. It should be noted that this polymer's absorption spectra largely resemble those of its corresponding oligomers of large *n*.[15] The energetic spacing between the vibronic levels here is 0.18 eV in all cases. Thickness measurement yields value for the absorption coefficient ~10^5 cm^{-1}, which is similar to the absorption coefficient of P3HT.[22]

Figure 2b shows the band edge shift, $\Delta_{bandedge}$, in PTV-0:10 (regioregular, red) and PTV-5:5 (regiorandom, black) upon going from film (line) to solution (symbol). In the case of PTV-0:10, $\Delta_{bandedge}$ is 0.07 eV, whereas in PTV (5:5), $\Delta_{bandedge}$ = 0.17 eV to the blue. The inset of Figure 2b is the plot of $\Delta_{bandedge}$ vs regioregularity (RR), and a trend of reduced $\Delta_{bandedge}$ with increased RR was observed, which means more ordered arrangement of side chains prevents coils of polymer backbones in solution. The fact that the vibronic levels are as well resolved in film as in solution suggests most chains are well separated and ordered in these films.

The exception of PTV-4:6 is rather puzzling. At first, it was expected that this was due to aggregation, as this material shows poorer film morphology than the others, characterized by visible aggregates and surface roughness. However, the fact that we do not observe a reduced slope of the band edge in PTV-4:6 compared with others indicates disorder alone cannot explain the resemblance of PTV-4:6 to PTV-0:10.[29] In light of this, there exists the possibility of block copolymer formation during the synthesis, although the relative reactivity of the two monomers used is similar, so efficient copolymer formation is not expected.[23] Perhaps the arrangement of the long alkyl chain relative to the thienylenevinylene unit assists in block copolymerization. Currently, investigations are underway to understand the strange behavior of this particular material.

The well-defined vibronic structure is further elucidated in Figure 3, where the thermal modulation of absorption (TMA) is shown. Figure 3a shows the absorption of PTV-0:10 at both 300 K (room temperature, RT) and 10 K, along with the resulting differential spectrum, which is calculated by $(T(\mathrm{RT}) - T(10\ \mathrm{K}))/T(10\ \mathrm{K})$. The band edge red-shifts 0.06 eV as the sample is cooled to 10 K. The minima in the differential spectrum (black arrows) correspond with the vibronic peaks at room temperature (RT), whereas the maxima (red arrows) show these at 10 K. The phonon energy which defines the vibronic levels in this polymer was 0.18 eV at room temperature and slightly smaller (0.17 eV) at 10 K. Our result is consistent with the previous publication about PTV.[30] Table 1 listed these replica energies. In comparing the TMA of all PTV-CRs (Figure 3b), it is seen that the minima are sharper and more easily resolved in the more regioregular polymers (PTV-0:10, 1:9, 2:8). Additionally, the magnitude of the 0−0 peak at 10 K for the regiorandom PTV-5:5 (truncated in Figure 3b) is much larger than for the others, indicating that this polymer is much more susceptible to thermal perturbation and has larger electron−phonon interaction, maybe due to the easier deformation of polymer backbones from less regular side chain

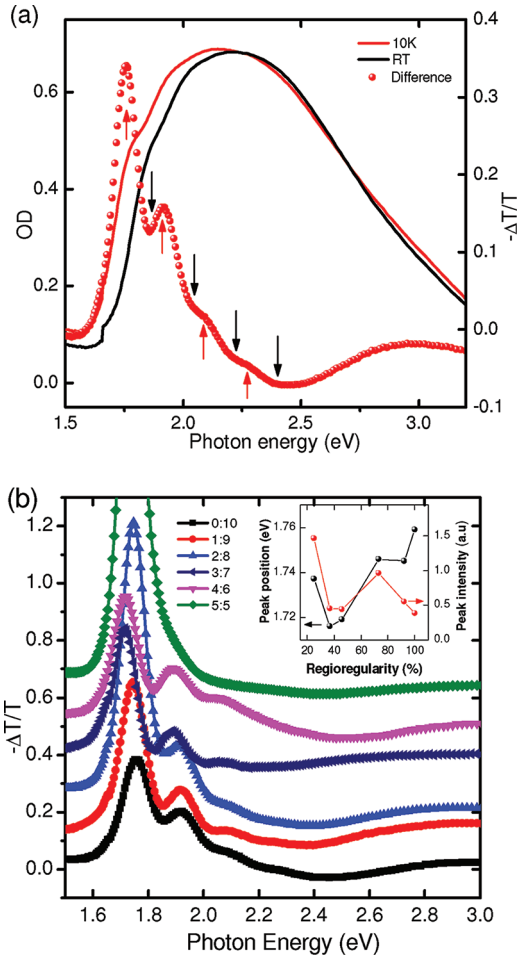

Figure 3. (a) Thermally modulated absorption (TMA) of PTV-0:10 film (red solid circle) obtained by $[T(\mathrm{RT}) - T(10\ \mathrm{K})]/T(10\ \mathrm{K})$. Also shown are the absorption spectra at RT (black line) and 10 K (red line). (b) A comparison of the TMA for all six PTV-CRs. The inset was the variation of 0−0 transition at 10 K versus regioregularity (peak position, black circle; peak intensity, red circle).

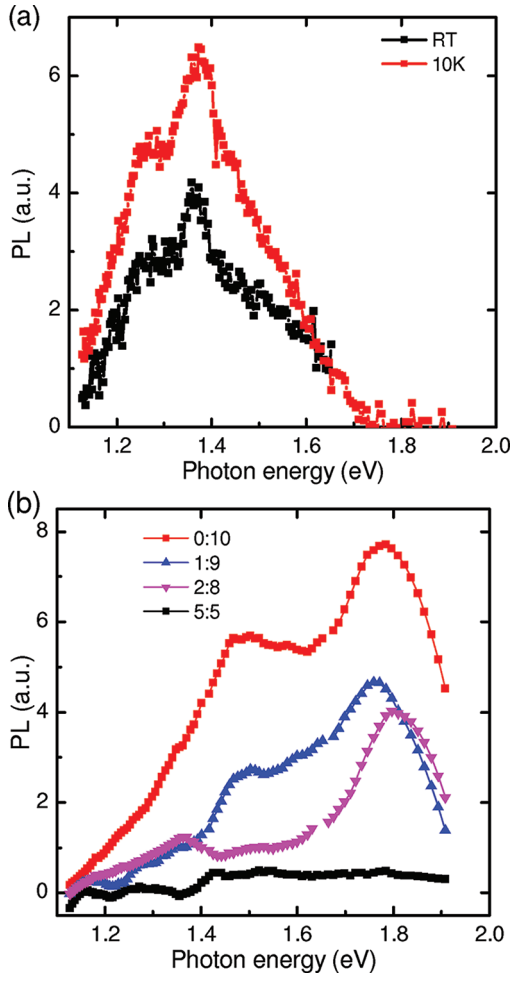

Figure 4. (a) PL of PTV- 0:10 (regioregular) film at room temperature (black line + solid square) and 10 K (red line + solid square). (b) PL of four PTV-CRs in dilute dichlorobenzene solution (0.01 mg/mL).

Table 1. Various Vibronic Replicas in Absorption of PTV-0:10 at RT (300 K) and Low Temperature (10 K)

temperature	0−0	0−1	0−2	0−3
RT (300 K)	1.75 eV	1.91 eV	2.08 eV	2.26 eV
low T (10 K)	1.85 eV	2.03 eV	2.21 eV	2.39 eV

arrangement. The inset of Figure 3b shows the variation of 0−0 peak versus regioregularity. As can be seen, while the peak position blue shifts, the peak intensity decreases, with increased regioregularity.

2. Photoluminescence. For the PTV-CRs studied here, only the regioregular PTV- 0:10 has measurable PL in solid state, with photoluminescence quantum efficiency (PLQE) $\sim 10^{-4}$. Figure 4a shows the PL of PTV- 0:10 film at room temperature (300 K) and low temperature (10 K). Both PL contains one peak (0−0) at 1.27 eV and another peak (0−1) at 1.38 eV, as well as a broad shoulder around 1.52 eV. There is negligible variation of PL with temperature, meaning that nonradiative recombination mechanisms such as phonon emission or disorder/defects/traps do not play an important role, as with most polymers.[29,30] Interchain interaction was also not a factor, as in the case of P3HT.[25,31] Other mechanism such as oxidization of thiophene rings was invoked to explain weak PL in PTV.[32] However, we have measured the PL of fresh and aged PTV- 0:10 and found no significant change in terms of both spectra and PLQE.

Figure 4b shows the PL of PTV-CR in very dilute dichlorobenzene solution (0.01 mg/mL) and PLQE $\sim 2 \times 10^{-4}$ for PTV- 0:10 (regioregular), whereas PLQE $< 10^{-5}$ for PTV- 5:5 (regiorandom). Therefore, the weakness of PL cannot be caused by the film quality,[30] but rather is *intrinsic* in nature. To explain the small PLQE in PTV within Kasha's rule, the photogenerated $1B_u$ exciton should undergo an internal conversion into a "dark" exciton with smaller energy.[33] According to the selection rules in π-conjugated polymers, the dark exciton should be an even-parity state ($2A_g$).[34] We thus conclude that the dark exciton in PTV-CR is in fact the $2A_g$ state, which has been extensively discussed in the literature in relation with the photophysics of π-conjugated polymers and oligomers.[16,33,34] Particularly, electroabsorption of PTV synthesized by thermal conversion of precursor polymer gave supportive evidence of the $2A_g$ exciton being below $1B_u$.[35] As a matter of fact, it is no surprise that the lowest-lying exciton in PTV is the dark $2A_g$. It turns out that any

replacement of the C═C double bond in polyacetylene, the simplest conjugated polymer, by other groups (i.e., phenylene, thienylene, triple bond, etc.) will increase the overall dimerization of the polymers and therefore increase the dimerization contribution to the optical band gap compared to the electron correlation contribution.[36] For small dimerization contribution to the optical gap, the system is highly correlated, and the $2A_g$ occurs below the $1B_u$. Conversely, for a large dimerization contribution, one-electron theory begins to win, and $2A_g$ is above the 1Bu. PTV and PT (polythiophene) are similar in the way that the replacement group is the same thienylene; however, PTV has a smaller dimerization contribution (alternate double bonds replaced by thienylene) compared to polythiophene (all double bonds replaced with thienylene). It was reported previously that the $2A_g$ is barely above the $1B_u$, and the order can easily be reversed via, for instance, modification of intermolecular interaction.[37] Another interesting point is that PTV has the same small gap of *trans*-polyacetylene (1.6 eV) and an even smaller gap than crystalline PTS-polydiacetylene.[38] Thus, the occurrence of the $2A_g$ here below the $1B_u$ is to be anticipated theoretically.

Comparing with film PL of PTV- 0:10, the solution PL also contains two peaks, one (0−0) at 1.48 eV and another (0−1) at 1.78 eV. The blue shift of 0−0 transition for 0.21 eV from dilute solution to film was expected, as the polymer chains go from isolated to close packed form, indicating the presence of energy transfer in the films. The Stokes shift for PTV- 0:10, Δ_s, was 0.60 eV for film and 0.48 eV for solution. The evolution of PL in solution with decreased regioregularity is very interesting. With reduced regioregularity, the relative oscillator strength of the 0−0 peak was also reduced, which might be due to more chain coil shortening the effective conjugation length of the polymer, and more emission would come from a shorter segment (at higher energy). PL completely vanished in the most random PTV- 5:5; therefore, we still observed the effect of disorder to increase the nonradiative recombination in PTV-CRs. Not only so, the formation of long-lived triplets was more pronounced in the more random PTV-CR, which further quenches PL, as will be explained in Figure 6.

3. Grazing Incidence X-ray Diffraction (GIXRD). The effect of alkyl side group arrangement on the polymer chain packing in film has been investigated by Grazing Incidence X-ray Diffraction (GIXRD). The results are displayed in Figure 5. There is no correlation between crystallinity and regioregularity (RR) (Table 2). This is, again, contrary to the case for poly(3-alkylthiophenes) (P3HT), where XRD peaks are only observed in RR-P3HT film.[39] The structural rigidity provided by the vinylene linkage of thiophene rings could be responsible for the crystalline order despite the randomly oriented alkyl chains. Regioregularity in PTV-CR is interesting for this reason because even the random films show microscopic order, and the second order effect of RR can be studied. The interchain distance inferred from the position of the first XRD peak (Table 2) is less than that of polythiophene derivatives of similar chain length.[39] In fact, the chains in PTV-CR are much closer together than those of poly(3-dodecylthiophene) which has the same alkyl side chain and is just slightly farther apart than those of poly(3-hexylthiophene).[39] This is significant, as it shows that the lack of interchain interaction in this material cannot be accounted for by the long alkyl group length. The inset of Figure 5 shows the dependence of interchain distance, *d*, and crystalline domain size versus RR. There seems to be no correlation between *d* and RR; however, we do observe reduced crystalline domain size as RR

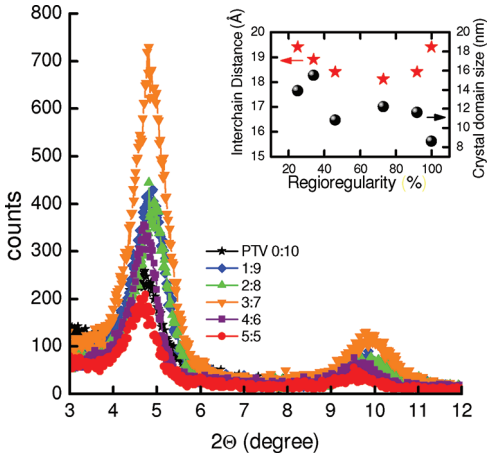

Figure 5. Grazing incidence X-ray diffraction measured in the out-of-plane geometry for all six polymers in this study. The inset shows the crystallinity (crystal size, solid circle; interchain distance, solid star) variation of regioregularity.

increases. The difference between PTV-CR and the well-studied P3HT implicates that different approaches and handling of PTV-CR are required for device applications, and further research into this direction is needed for any significant improvement of PTV solar cell performance.

4. Photoinduced Absorption (PIA) and Doping-Induced Absorption (DIA). The photoinduced absorption (PIA) spectra of PTV-CRs are displayed together in Figure 6a. The PIA spectra contain three main PA bands: P_1 (∼0.33 eV), P_2 (∼0.93 eV), and T (∼1.2 eV). P_1 is due to a transition from the highest occupied molecular orbital (HOMO) to a midgap state, whereas P_2 is due to a transition between two midgap states (Figure 6b). The higher energy peak, T, is attributed to the formation of long-lived triplet excitons by intersystem crossing or by singlet exciton fission.[25,40] P_1 and P_2 are correlated to each other since they show similar recombination dynamics, as verified by measuring their dependencies on the laser excitation intensity and modulation frequency (see Figure 8). In contrast, the PIA band denoted T in Figure 6a does not correlate with P_1 and P_2; its spectrum is much sharper and is absent in the quadrature PIA spectrum, showing that it is much faster than P_1 and P_2. Also the PIA shoulder at the polymer band edge (∼1.6 eV) may be due to electro-absorption photogenerated charge excitations and thermal modulation (see Figure 3). PB at $h\omega(probe) >$ ∼1.6 eV is photobleaching of the ground state absorption. Figure 6b shows the energy diagrams of the most important excited states and related optical transitions in the neutral (triplet) and charge manifolds.

At the band edge, a strong oscillatory behavior is observed which is most likely due to thermal modulation, of the kind discussed in Figure 3, induced by laser sample heating. Since the thermally modulated absorption is of order unity (Figure 3b), this would account for the large magnitude of these oscillations as compared to that of the PIA which is of the order of 10^{-4}. However, a superimposed Frank−Keldysh band edge oscillation due to the presence of the charged polarons on the chain cannot be ruled out.[41] Currently, electroabsorption (EA) measurements are underway to determine if this is the case.

To further identify the various PIA bands, we measured the doping-induced absorption (DIA) by exposing the PTV films to iodine vapor.[42] In Figure 7, two DIA bands are observed for each

Table 2. Summary of GIXRD Data for PTV-CR

PTV-C12-*a*:*b*	2θ peak position (degrees)[a]	2θ peak width (fwhm, degree)	interchain distance (Å)	domain size (nm)
0:10	4.64	1.04	19.4	8.6
1:9	4.82	0.763	18.4	11.6
2:8	4.89	0.721	18.1	12.2
3:7	4.82	0.817	18.4	10.8
4:6	4.71	0.565	18.9	15.5
5:5	4.63	0.643	19.4	13.9

[a] Position of the first-order 2θ peak in Figure 5 was determined by a Gaussian fit.

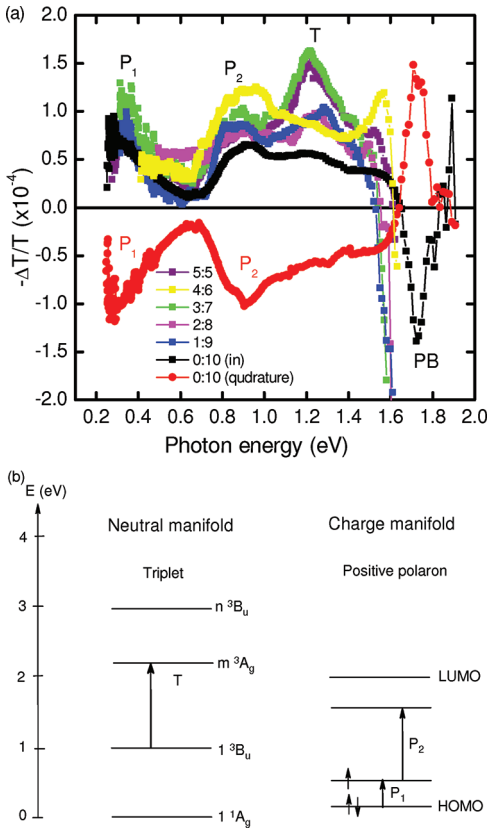

Figure 6. (a) PIA spectra of all six PTV-CRs. The excitation is the 457 nm line from an Ar^+ laser at an intensity of 100 mW/cm^2. The sample is held at a temperature of 10 K. (b) Schematic energy diagram of the most important excited states in PTV-CR and related optical transitions in the neutral triplet manifold and charge manifold for a positive polaron.

polymer, which are accompanied by infrared-active vibrations (IRAVs), thus confirming that they are indeed due to charged excitations.[43] From the two DIA bands, we conclude that the charge excitations in PTV-CR are *polarons*[44] and therefore identify P_1 and P_2 bands in the PIA spectrum (Figure 6a) as due to long-lived polaron photoexcitations. The DIA bands appear at higher energies than P_1 and P_2 bands upon photoexcitation (Figure 6a); this is due to "pinning" by the accompanying dopant ion having opposite charge.[45] In contrast, the band T in the PA spectrum is not correlated with the DIA bands and is therefore due to long-lived *neutral* excitations, which we thus identify as triplet excitons. Recent work on oligothienylenevinylenes (OTV)

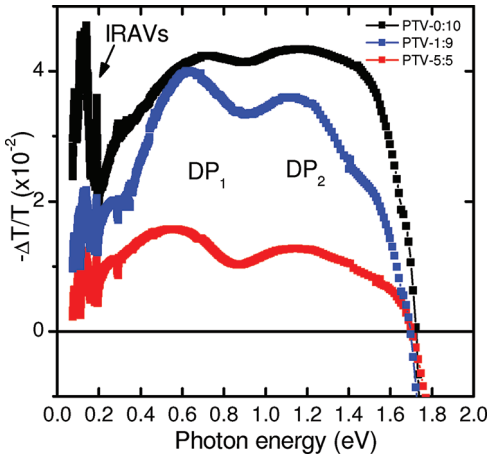

Figure 7. Doping-induced absorption (DIA) spectra of of PTV-CRs with three regioregularities. Polaron absorption bands (DP_1 and DP_2) and correlated IR-active vibrations (IRAVs) were shown.

has confirmed the triplet absorption at 1.42 eV for 12 units of OTV with a triplet state at about 1.06 eV.[16] We therefore estimate that the triplet 1^3B_u level for PTV is at 1.0 eV (Figure 6b). Further experimental work is ongoing to determine the exact value of this state.

As for the assignment of the photoexcited species, not only does the sharper spectral shape of the 1.2 eV (band T) distinguish it from the other two PIA bands (P_1 at 0.33 eV, P_2 at 0.93 eV) but also in Figure 8a we show that the dependence of the PIA of band T on pump intensity, I, indicates that its recombination dynamics is different from that of P_2. P_1 has similar dependence as P_2, and therefore the data of P_1 are not shown here. Both polaron and triplet photoexcitations exhibit nearly square-root dependencies for pump intensity above 50 mW/cm^2 (fit using $\Delta T \sim I^m$, where the exponent m = 0.43 and 0.39 for triplets and polarons, respectively); however, at low laser excitation intensity, the polaron band is superlinear, whereas the triplet band shows sublinear dependence. The deviation from linearity in the near steady state conditions (low modulation frequency) is a signature of a bimolecular recombination mechanism.[46] For this reason, both types of photogenerated species in PTV recombine bimolecularly. Bimolecular recombination is not as common for triplets but has been observed before and was interpreted as evidence of triplet−triplet annihilation.[46,47]

In light of these assignments, it is notable that the formation of triplets is more efficient in the more random polymers PTV-3:7 and PTV-5:5 (again, PTV-4:6 behaves more like a regioregular polymer). The reduced triplet formation in more regular PTV-CR is in consistency with photoluminescence quantum efficiency (PLQE, η) results. For the most regular PTV-0:10, $\eta \sim 2 \times 10^{-4}$ and $\eta < 10^{-5}$ (the instrument limit) for the most random PTV-5:5. The results displayed here show that the effect of side chain arrangement in film can be crucial to the fundamental properties (i.e., triplet formation) of π-conjugated polymers. In this case, the PIA spectra of random PTV-5:5 is similar to that of its parent polymer synthesized by thermal conversion of precursor polymers, where photoexcitations are expected to be of an intrachain character.[30] The strongest effect of regioregularity observed in PTV-CR is the suppression of a triplet state which depends on the placement of the $1B_u$ and $2A_g$ levels. Such an effect does not even require an interchain interaction. This property of

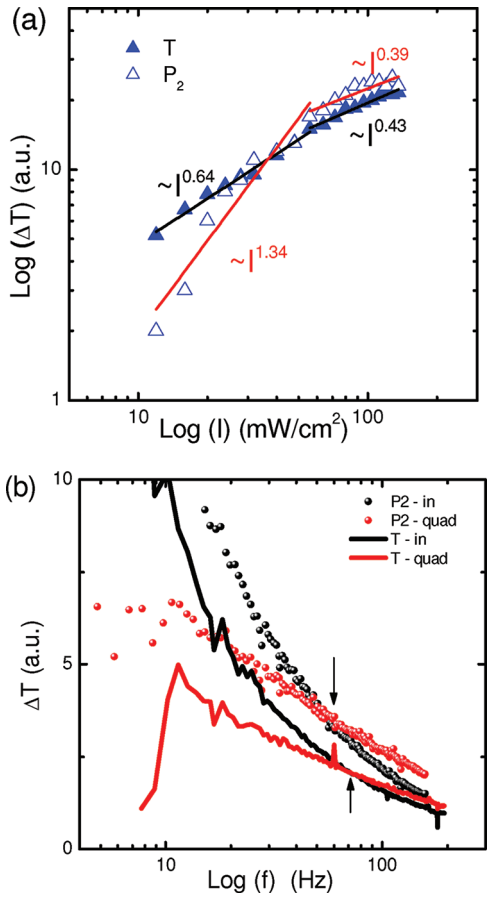

Figure 8. (a) Pump intensity dependence of PIA of PTV-1:9 measured at a modulation frequency of 30 Hz. Filled triangles are for the triplet excitation, T; open triangles are for the polaron P_2. The lines indicate linear fitting of experimental data based on $\Delta T \sim I^m$. (b) The frequency dependence of PIA on PTV-5:5 for P_2 (solid circles) and T (solid lines) measured both in-phase (black) and in quadrature (red). The laser intensity is 40mW/cm^2. In both cases, the sample is at 10 K while under illumination with the 457 nm line from an Ar^+ laser.

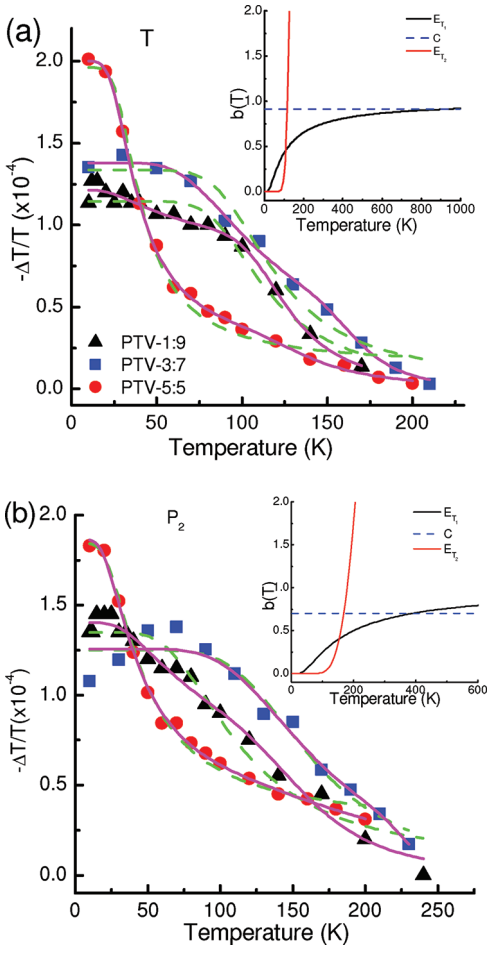

Figure 9. Temperature dependence of the PIA bands of the films for PTV-1:9 (triangles), PTV-3:7 (squares), and PTV-5:5 (circles). The triplet exciton band, T, is shown in (a), while the polaron band, P_2, is shown in (b). The fittings using eq 3 were shown as a magenta solid line for two activation energies and a green broken line for one activation energy. The insets show the decay rate $b(T)$ with a shallow trap (black line) and deep trap (red line) for (a) triplet band T and (b) polaron band P_2. The blue broken line indicates the temperature-independent part C in eq 3.

PTV-CR suggests RR will likely be necessary to aid in electron transfer with n-type fullerenes if it is to be useful in OPV application.

In Figure 8b, the dependence of the PIA on the pump modulation frequency, f, shows that the long-lived photoexcitations in PTV-CR have lifetimes on the order of a millisecond, as extracted from the crossing point frequency of the in-phase and quadrature PIA signals.[24,46] Although the lifetimes of P_2 and T are similar, they are not identical. The triplet has a lifetime 1.3 times shorter than that of P_2. In random PTV-5:5, these lifetimes are 2.4 and 3.2 ms, respectively, whereas they are 4.7 and 5.7 ms, respectively, in regular PTV-0:10. The longer lifetime of these species as the regioregularity increases indicates a decrease in the density of recombination centers in the more ordered polymer.

Figure 9 shows the temperature dependence of the PIA bands, namely, P_2 (0.93 eV) and T (1.2 eV), for three PTV-CR films. The measurement was done with low pump intensity and slow modulation frequency f ($1/f \gg \tau_T$ and τ_{P2}). At higher temperatures, the decay of the PIA is due to thermal depopulation of the defect states and can be related to the trap energy depth. The triplet (T) absorption (Figure 9a) decays monotonically with a plateau region at low temperature. For PTV-5:5, the decay is very fast, which confirms the thermal sensitivity of the most random polymer; the plateau extends out to 75 K for PTV-3:7 and to nearly 100 K for PTV-1:9. To further understand the triplet kinematics, the experimental data were fit using a thermal activation model for traps in polymers.[48] The lines in Figure 9 showed the results of fitting. The density of long-lived photoexcitations n_{ss} at steady-state condition ($1/f \gg \tau$, where τ is the lifetime of the photoexcitation) is expressed by

$$n_{ss} = (aG/b)^{1/\mu} \quad (1)$$

where G is the pump light intensity and a is the generation rate, usually a constant with constant G. b is the recombination (decay) rate and is dependent on temperature and light intensity. Under constant illumination of pump light, $b = b(T)$ mainly varies with temperature T. μ is between 1 (monomolecular recombination) and 2 (bimolecular recombination) and can be obtained by the dependence of PIA signal on pump intensity (Figure 8). Under a pump intensity of 40 mW/cm^2, μ was determined to be 0.64 for triplet (see Figure 8a). Under constant

dx.doi.org/10.1021/jp2066666 |J. Phys. Chem. B 2011, 115, 13139–13148

Table 3. Summary of Fitting Results Using Equation 3 for Triplet Band T

PTV-CR	number of activation energies	E_{T_1} (meV)	E_{T_2} (meV)	C (temperature independent)	B (weight of E_{T_2})
PTV- 1:9	2	7.4 ± 2.3	103 ± 16.0	0.91 ± 0.34	$(2.5 \pm 3.2) \times 10^4$
	1	61 ± 9.7		$(1.3 \pm 1.3) \times 10^{-3}$	
PTV- 3:7	2	35 ± 5.0	227 ± 71.0	0.02 ± 0.01	$(8.5 \pm 3.8) \times 10^5$
	1	63 ± 11		$(1.4 \pm 1.3) \times 10^{-3}$	
PTV- 5:5	2	12 ± 0.40	104 ± 21.0	0.02 ± 0.002	$(2.5 \pm 3.7) \times 10^3$
	1	15 ± 1.2		0.01 ± 0.003	

Table 4. Summary of Fitting Results Using Equation 3 for Polaron Band P_2

PTV-CR	number of activation energies	E_{T_1} (meV)	E_{T_2} (meV)	C (temperature independent)	B (weight of E_{T_2})
PTV- 1:9	2	12 ± 3.0	84 ± 22	0.70 ± 0.31	225 ± 266
	1	31 ± 4.0		0.07 ± 0.03	
PTV- 3:7	2[a]	57 ± 19	442 ± 1843	0.03 ± 0.04	$(1.7 \pm 16) \times 10^8$
	1	64 ± 12		0.02 ± 0.01	
PTV- 5:5	2	7.5 ± 0.4	68 ± 37	0.33 ± 0.03	14 ± 29
	1	8.3 ± 0.4		0.28 ± 0.02	

[a] The fitting result of PTV- 3:7 using two activation energies was very poor.

pump intensity, eq 1 can be written as

$$n_{ss} \propto b(T)^{-1/\mu} \quad (2)$$

where $b(T)$ is usually described by a thermal activation behavior, with the activation energy E_T of the trap state extracted from a fitting using

$$n_{ss}(T) = A(e^{(-E_{T_1}/k_B T)} + Be^{(-E_{T_2}/k_B T)} + C)^{-1/\mu} \quad (3)$$

where A is a scaling factor; E_{T_1} and E_{T_2} are the thermal activation energies for two trap states; B represents the relative weight of the E_{T_2} activated process; and C is the T-independent part of the decay rate. When B is set to zero, the fitting was done using only one activation energy. The fitting results were shown in Figure 9 as a magenta solid line (two activation energies) and a green broken line (one activation energy). For triplet T (Figure 9a), better fitting was done using two activation energies, i.e., one shallow trap (E_{T_1} < 50 meV) and one deeper trap (E_{T_2} > 100 meV), for all three PTV-CRs. It can be seen that at T < 100 K the shallow trap dominates the recombination of triplets. At higher temperature, the deeper trap above 100 meV dominates the recombination. That is why using one activation energy resulted in an increase of error at higher temperature (T > 120 K). The parameter B was at the order of 10^3 to 10^6 for the three PTV-CRs, indicating a significant influence from the deeper trap. The fitting does not show a correlation between regioregularity and the trap state depth (or activation energy). Table 3 gave a detailed summary of the fitting results.

However, the decay rate does show correspondence with regioregularity. The most random PTV- 5:5 has the fastest decay, as indicated by the least plateau region. We explain this by increased nonradiative recombination due to defects such as chain kinks in the least structurally ordered PTV- 5:5 film. The nonradiative decay further increases the decay rate of photoexcitations. This also explains the shorter lifetime of polarons and triplets in the PTV- 5:5 film (Figure 8).

Figure 9b shows the temperature dependence of P_2 (0.93 eV). Fitting of experimental data using eq 3 was shown as a magenta solid line (two activation energies) and a green broken line (one activation energy). Using two activation energies, the fitting of PTV- 5:5 gave a good result, with a shallow trap at 7.5 meV and a deeper trap at 68 meV. However, the fitting results of PTV- 1:9 and PTV- 3:7 did not go very well with the experimental curves, especially at the low-temperature region (T < 100 K). At this region, the polaron excitation exhibits a very interesting feature for these two more regular polymers. An increase in the PIA signal with increasing temperature is apparent. PTV- 3:7 shows a strong increase in the PIA signal until it peaks near 70 K. On the other hand, PTV- 1:9 shows a smaller increase at about 20 K and a plateau region at 70 K. We think there are two possible mechanisms for the increase. One is due to thermally enhanced polaron generation. In this process, the molecular resonance barrier is reduced as the temperature is raised, and the chain becomes less resistive to the polaronic chain deformation. The other is the thermally activated triplet dissociation. The triplets at the shallow trap sites could dissociate into two polarons due to thermal perturbation. Noticeably, the temperature variation of the triplet for PTV- 0:10 and PTV- 3:7 was much flatter in the low-temperature region (Figure 9a). The competing polaron generation gave way to the thermally activated recombination of polarons at temperature higher than 20 K for PTV- 1:9 and 75 K for PTV- 3:7. As a matter of fact, the superlinear increase in P_2 absorption with increasing pump intensity at the low intensity region (Figure 8a) may also be due to thermally enhanced polaron generation as increased pump fluence leads to sample heating. The thermally enhanced polaron generation was not observed with the most random PTV- 5:5, and since this polymer has much smaller activation energy for polaron (Table 4), the thermal perturbation likely annihilated the polarons. In addition, the disorder-related nonradiative decay might have canceled out the enhancement at low temperature for this polymer.

The inset of Figure 9b shows the decay rate $b(T)$ of polaron with a shallow trap (black line) and deep trap (red line). It can be seen that at T < 150 K the shallow trap dominates the recombination of polarons. At higher temperature, the deeper trap above 90 meV dominates the

recombination. Table 4 summarizes the detailed fitting results for polaron thermal decay. Overall, polarons have lower activation energy than triplets in this series of polymers, regardless of regioregularity.

CONCLUSIONS

Using continuous wave photoinduced absorption (cw-PIA), doping-induced absorption (DIA), and thermally modulated absorption (TMA), the optical properties of poly(3-dodecylthienylenevinylene) with controlled regioregularity (PTV-CR) in the broad spectrum range from UV to near IR have been studied. We found that regioregularity affects the photophysics of PTV-CR in a different way than that with poly(3-alkylthiophene). The optical bandgap increases with regioregularity from 1.65 to 1.75 eV for the most random PTV- 5:5 (head−tail ratio of 25%) to regular PTV- 0:10 (head−tail ratio of 100%). We found that PTV-CR is intrinsically *dark* with very small PL quantum efficiency ranging from 10^{-5} to 2×10^{-4}, from most random PTV- 5:5 to regular PTV- 0:10. We attribute the nonluminescent property to the existence of the dark excitonic state ($2A_g$) which lies below the bright excitonic state ($1B_u$). The phonon level in all PTV-CRs is about 0.18 eV and bears temperature invariance. The side chain arrangement seems to have little influence over film morphology, as indicated by the GIXRD results of crystallinality and domain size. There is no correlation between structure order and regioregularity in PTV-CR, in contrast with the case of poly(3-alkylthiophene). The measured cw-PIA and doping-induced absorption spectra confirm that the long-lived charged and neutral photogenerated species are polarons and triplet excitons, respectively, and thus PTV-CR is a *unique* nondegenerate ground state π-conjugated polymer which is intrinsically nonluminescent. Through the measurements and the analysis of the PIA signal dependency on pump intensity, frequency, and the temperature of the sample, the respective recombination and generation mechanisms of polarons and triplets were characterized.

Our studies of side chain organization effect on films of PTV-CR provide a new perspective into regioregularity as a means of improving optoelectronic properties of π-conjugated polymers for device applications. Since very little to no evidence of interchain interaction, despite the fact that the polymer chains are reasonably close together as shown in GIXRD, has been observed even in the most regioregular polymers, subtle effects of chain organization on intrachain, one-dimensional (1D) excitations have been revealed. The results here suggest that regioregular self-assembly may not only improve mobility and photon harvesting, as observed elsewhere, but also be necessary for quenching dissipative channels that will inhibit electron transfer in heterojunction type OPVs in the case of novel polymers such as low band gap PTV-CR.

AUTHOR INFORMATION

Corresponding Author

*E-mail: xjiang@usf.edu. Phone: (813) 974-7765. Fax: (813) 974-5813.

ACKNOWLEDGMENT

The authors thank Dr. S.−S. Sun at Norfolk Sate University for supplying some of the materials used in this study. The XRD measurements were performed at the Nanotechtology Research and Education Center (NREC) at University of South Florida, and in particular Robert Tufts has been helpful in providing access and support. Financial support has been provided by New Energy Technology, Inc. The authors also thank Prof. Z. V. Vardeny for helpful comments and discussions.

REFERENCES

(1) Ma, W.; Yang, C.; Gong, X.; Lee, K.; Heeger, A. J. *Adv. Funct. Mater.* **2005**, *15*, 1617–1622.
(2) Reyes-Reyes, M.; Kim, K.; Carroll, D. L. *Appl. Phys. Lett.* **2005**, *87*, 083506–083508.
(3) Z. Bao, Z.; A. Dodabalapur, A.; Lovinger, A. J. *Appl. Phys. Lett.* **2006**, *69*, 4108–4110.
(4) Shaheen, S. E.; Brabec, C. J.; Sariciftci, N. S.; Padinger, F.; Fromherz, T.; Hummelen, J. C. *Appl. Phys. Lett.* **2001**, *78*, 841–843.
(5) Morgado, J.; Friend, R. H.; Cacialli, F. *Appl. Phys. Lett.* **2002**, *80*, 2436–2438.
(6) Roncali, J. *Chem. Rev.* **1997**, *97*, 173–206.
(7) Zhang, C.; Matos, T.; Li, R.; Annih, E.; Sun, S.; Lewis, J. E.; Zhang, J; Jiang, X. *Polym. Chem.* **2010**, *1*, 663–669.
(8) Banishoeib, F.; Henckens, A.; Fourier, S.; Vanhooyland, G.; Breselge, M.; Manca, J.; Cleij, T. J.; Lutsen, L.; Vanderzande, D; Nguyen, L. H. *Thin Solid Films* **2008**, *516*, 3978–3988.
(9) Fuchigami, H.; Ysumura, A.; Koezuka, H. *Appl. Phys. Lett.* **1993**, *63*, 1372–1374.
(10) Liang, Y. Y.; Xu, Zheng; Xia, J. B.; Tsai, Sl; Wu, Y.; Li, G.; Ray, C.; Yu, L. P. *Adv. Mater.* **2010**, *22*, E135–E138.
(11) Li, Y. F.; Zou, Y. P. *Adv. Mater.* **2008**, *20*, 2952–2958.
(12) Girotto, C; Cheyns, D; Aernouts, T; Banishoeib, F; Lutsen, L; Cleij, T. J.; Vanderzande, D; Genoe, J; Poortman, J; Heremans, P. *Org. Electron.* **2008**, *9*, 740–746.
(13) Nguyen, L. H.; Gunes, S; Neugebauer, H; Sariciftci, N. S.; Banishoeib, F; Henckens, A; Cleij, T; Lutsen, L; Vanderzande, D *Solar Energy Mater. Solar Cells.* **2006**, *90*, 2815–2828.
(14) Smith, A. P.; Smith, R. R.; Taylor, B. E.; Durstock, M. F. *Chem. Mater.* **2004**, *16*, 4687–4692.
(15) Jestin, I.; Frere, P.; Mercier, N.; Levillain, E.; Stievenard, D.; Roncali, J. *J. Am. Chem. Soc.* **1998**, *120*, 8150–8158.
(16) Apperloo, J. J.; Martineau, C.; van Hal, P. A.; Roncali, J.; Janssen, R. A. J. *J. Phys. Chem. A* **2002**, *106*, 21–31.
(17) Hwang, I; Xu, Q; Soci, C; Chen, B; Jen, A; Moses, D; Heeger, A. J. *Adv. Funct. Mater.* **2007**, *17*, 563–568.
(18) Kim, J; Qin, Y; Stevens, D; Ugurlu, O; Kalihari, V; Hillmyer, M; Frisbie, C *J. Phys. Chem. C* **2009**, *113*, 10790–10797.
(19) Prosa, T. J.; Winkour, M. J.; McCullough, R. D. *Macromolecules* **1996**, *29*, 3654–3656.
(20) Sirringhaus, H; Brown, P. J.; R. H. Friend, R. H.; Nielsen, M. M.; K. Bechgaard, K; Langeveld-Voss, B. M. W.; Spiering, A. J. H.; Janssen, R. A. J.; Meijer, E. W.; Herwig, P; de Leeuw, D. M. *Nature* **1999**, *401*, 685–687.
(21) Korovyanko, O. J.; Österbacka, R.; Jiang, X. M.; Vardeny, Z. V.; Janssen, R. A. J. *Phys. Rev. B* **2001**, *64*, 235122.
(22) Kim, Y; Cook, S; Tuladhar, S. M.; Choulis, S. A.; Nelson, J; Durrant, J. R.; Bradley, D. D. C.; Giles, M; McCulloch, I; Ha, C; Ree, M *Nat. Mater.* **2006**, *5*, 197–203.
(23) Zhang, C.; Sun, J.; Li, R.; Sun, S.; Lafalce, E.; Jiang, X. *Macromolecules* **2011**, *44*, 6389–6396.
(24) Vardeny, Z. V.; Wei, X. In *Handbook of Conducting Polymers*, 2nd ed.; 2007; pp 639 − 666.
(25) Jiang, X. M.; Österbacka, R; Korovyanko, O. J.; An, C. P.; Horovitz, B; Janssen, R. A. J.; Vardeny, Z. V. *Adv. Funct. Mater.* **2002**, *12*, 587–597.
(26) deMello, J. C.; Wittmann, H. F.; Friend, R. H. *Adv. Mater.* **1997**, *9*, 230–240.
(27) Österbacka, R.; An, C. P.; Jiang, X. M.; Vardeny, Z. V. *Science* **2000**, *287*, 839–842.

(28) Sexias de Melo, J.; Silva, L. M.; Arnaut, L. G. *J. Chem. Phys.* **1999**, *111*, 5427–5433.
(29) Clark, J.; Silva, C.; Friend, R. H.; Spano, F. C. *Phys. Rev. Lett.* **2007**, *98*, 206406–4.
(30) Brasset, A. J.; Colaneri, N F.; Bradley, D. D. C.; Lawrence, R. A.; Friend, R. H. *Phys. Rev. B* **1990**, *41*, 10586–10594.
(31) Brown, P. J.; Thomas, D. S.; Kohler, A; Wilson, J. S.; Kim, J. S.; Ramsdale, C. M.; Sirringhaus, H; Friend, R. H. *Phys. Rev. B* **2003**, *67*, 064203–14.
(32) Jeeva, S.; Lukoyanova, O.; Karas, A.; Dadvand, A.; Rosei, F.; Perepichka, D. F. *Adv. Funct. Mater.* **2010**, *20*, 1661–1669.
(33) Soos, Z. G.; Elemad, S.; Galvão, D. S.; Ramasesha, S. *Chem. Phys. Lett.* **1992**, *194*, 341–346.
(34) Dixit, S. N.; Guo, D.; Mazumdar, S. *Phys. Rev. B* **1991**, *43*, 6781–6784.
(35) Liess, M.; Jeglinski, S; Vardeny, Z. V.; Ozaki, M; Yoshino, K; Ding, Y; Barton, T. *Phys. Rev. B* **1997**, *56*, 15712–15723.
(36) Soos, Z. G.; Ramasesha, S.; Galvão, D. S. *Phys. Rev. Lett.* **1993**, *71*, 1609–1612.
(37) Periasamy, N.; Dianieli, R.; Ruani, G.; Zamboni, R.; Taliani, C. *Phys. Rev. Lett.* **1992**, *68*, 919–922.
(38) Robins, L.; Orenstein, J.; Superfine, R. *Phys. Rev. Lett.* **1986**, *56*, 1851–1853.
(39) Chen, T. A.; Wu, X.; Rieke, R. D. *J. Am. Chem. Soc.* **1995**, *117*, 233–244.
(40) Guo, J.; Ohkita, H.; Benten, H.; Ito, S. *J. Am. Chem. Soc.* **2009**, *131*, 16869–16880.
(41) Sebastian, L.; Weiser, G. *Phys. Rev. Lett.* **1981**, *46*, 1156–4.
(42) Deussen, M.; Bassler, H. *Synth. Met.* **1993**, *54*, 49–55.
(43) Ehrenfreund, E.; Vardeny, Z.; Brafman, O.; Horovitz, B. *Phys. Rev. B* **1987**, *36*, 1535–1553.
(44) Lane, P. A.; Wei, X.; Vardeny, Z. V. *Phys. Rev. Lett.* **1996**, *77*, 1544–4.
(45) Heeger, A. J.; Kivelson, S.; Schrieffer, J. R.; Su, W. P. *Rev. Mod. Phys.* **1988**, *60*, 781–851.
(46) Wohlgenannt, M.; Graupner, W.; Leising, G.; Verdeny, Z. V. *Phys. Rev. B* **1999**, *60*, 5321–5330.
(47) Lane, P. A.; Wei, X.; Vardeny, Z. V. *Phy. Rev. B* **1997**, *56*, 4626–4637.
(48) Graupner, W.; Leditzky, G.; Leising, G.; Scherf, U. *Phys. Rev. B* **1996**, *54*, 7610–7613.